Genomic Characterization of IMP-Producing Pseudomonas aeruginosa in Bulgaria Reveals the Emergence of IMP-100, a Novel Plasmid-Mediated Variant Coexisting with a Chromosomal VIM-4

Ivan Stoikov * , Ivan N. Ivanov , Deyan Donchev , Deana Teneva , Elina Dobreva , Rumyana Hristova , Stefana Sabtcheva

Posted Date: 31 July 2023

doi: 10.20944/preprints202307.2054.v1

Keywords: Pseudomonas; metallo-beta-lactamase; blaIMP; novel allele; plasmid

Article

Genomic Characterization of IMP-Producing *Pseudomonas aeruginosa* in Bulgaria Reveals the Emergence of IMP-100, a Novel Plasmid-Mediated Variant Coexisting with a Chromosomal VIM-4

Ivan Stoikov [1,2,*], Ivan N. Ivanov [1], Deyan Donchev [1], Deana Teneva [1], Elina Dobreva [1], Rumyana Hristova [1] and Stefana Sabtcheva [2]

[1] National Reference Laboratory for Control and Monitoring of Antimicrobial Resistance, Department of Microbiology, National Center of Infectious and Parasitic Diseases, 26 Yanko Sakazov Blvd. 1504 Sofia, Bulgaria

[2] Laboratory for Clinical Microbiology, National Oncology Center, 6 Plovdivsko pole Str. 1797 Sofia, Bulgaria

* Correspondence: ivanstoikovbt@gmail.com

Abstract: Multidrug-resistant (MDR) *Pseudomonas aeruginosa* infections represent major a public health concern and require comprehensive understanding of their genetic make-up. This study investigated the first occurrence of IMP-carrying MDR *P. aeruginosa* strains from Bulgaria. Whole genome sequencing identified a novel plasmid-mediated *bla*$_{IMP-100}$ allele located in a In1300-like integron embedded in a novel putative transposon. Two other closely related chromosomal bla$_{IMP}$ variants IMP-13 and IMP-84 were also detected. The IMP-producers were resistant to last-line drugs including cefiderocol (CFDC) (2 out of 3) and susceptible to colistin. The *bla*$_{IMP-13/84}$ cassettes were situated in a *In320* integron inserted in a *Tn5051*-like transposon as previously reported. Lastly, the p47825-IMP plasmid rendered PAO1 transformant resistant to CFDC, suggesting a transferable CFDC resistance. A variety of virulence factors associated with adhesion, antiphagocytosis, iron uptake, quorum-sensing, as well as secretion systems, toxins, and proteases were confirmed, suggesting significant pathogenic potential consistent with the observed strong biofilm formation. Emergence of IMP-producing MDR *P. aeruginosa* is alarming as they remain unsusceptible even to last geneneration drugs like CFDC. Newly detected IMP-100 was even located in an CFDC-resistant XDR strain.

Keywords: *Pseudomonas*; metallo-beta-lactamase; blaIMP; novel allele; plasmid

Introduction

Pseudomonas aeruginosa is a member of the ESKAPE group of highly resistant pathogens and represents a formidable challenge in healthcare settings (Daikos *et al.*, 2021). Carbapenems remain the mainstay for treating severe and complicated *P. aeruginosa* infections. Unfortunately, the emergence of carbapenem resistance has become a global concern in the last decade (Toleman *et al.*, 2005; Zavascki *et al.*, 2006), and is commonly associated with mutations in the outer-membrane porin OprD, overexpression of efflux pumps and horizontal acquisition of carbapenemase genes, including both serine- and metallo-β-lactamases (MBLs) (Walsh *et al.*, 2005; Quale *et al.*, 2006; Zavascki *et al.*, 2006; Rodríguez-Martínez, Poirel and Nordmann, 2009).

Carbapenemase activity in clinical strains *P. aeruginosa* due to KPC and certain GES variants (Ambler class A) is less frequently reported similar to the OXA carbapenemases from Ambler class D (Hong *et al.*, 2015). MBLs (Ambler class B) are characterized by their dependency on one or two zinc cations for enzymatic activity (Walsh *et al.*, 2005). Various types of MBLs have been identified in *P. aeruginosa*, including IMP, VIM, SPM, GIM, NDM, FIM, BIM types (Hong *et al.*, 2015; Souza *et al.*, 2023). Among these, IMP- and VIM-type enzymes are the most abundant and are of particular clinical importance, as they efficiently inactivate most β-lactam antibiotics, with the exception of monobactams (Gupta, 2008; Zhao and Hu, 2010).

 doi:10.20944/preprints202307.2054.v1

Integrons play a crucial role in capturing and disseminating antibiotic resistance genes including MBLs (Walsh et al., 2005) as they are often associated with large transposon structures found on plasmids or chromosomes (Mazel, 2006; Zhao and Hu, 2011). Transposable elements utilize specific transposase-mediated mechanisms for their insertion and excision within the bacterial genome. Composite transposons are flanked by Insertion Sequence (IS) elements. Unit transposons, on the other hand, encode an excision/integration-associated enzyme, recombinase or resolvase, along with accessory genes such as resistance genes, within a single genetic unit. Conjugative transposons, also referred to as integrative conjugative elements (ICEs), carry genes for excision, conjugative transfer, and integration, often accommodating a diverse repertoire of accessory genes, including antibiotic resistance genes (Roberts *et al.*, 2008).

The first identification of IMP-1 metallo-β-lactamase, conferring acquired resistance to carbapenems, was reported in 1988 in a *P. aeruginosa* strain isolated from Japan (Watanabe *et al.*, 1991). Since then the emergence and spread of *bla*$_{IMP}$-carrying *P. aeruginosa* strains has been reported globally (Wang *et al.*, 2021). The IMP-type enzymes represent a highly heterogeneous group of carbapenemases, frequently found as gene cassettes in class 1 integrons harboring additional resistance determinants (Walsh *et al.*, 2005; Zhao and Hu, 2011).

P. aeruginosa isolates in Bulgaria display a range of carbapenemases, of which VIM-type enzymes are commonly reported (Schneider *et al.*, 2008; Strateva, Setchanova and Peykov, 2021). Co-occurrence of NDM-1 and GES-5 carbapenemases were recently identified (Kostyanev *et al.*, 2020). Detection of OXA-50 carbapenemase has also been documented (Petrova *et al.*, 2019).

In this study, we performed genomic analysis of three clinical *P. aeruginosa* isolates, revealing to our knowledge the first occurrence of *bla*$_{IMP}$ in Bulgaria. In addition, one of the isolates carried a novel IMP-type metallo-β-Lactamase variant, referred to as *bla*$_{IMP-100}$, located on a multidrug-resistant plasmid and in combination with a chromosomally encoded *bla*$_{VIM-4}$.

Materials and methods

Strains

The three strains (Paer3541, Paer3796A, and Paer4782MK) were initially isolated in Sofia, Bulgaria between 2018 and 2022. Paer3541 was obtained from throat swab from hospitalized patient, Paer3796A was derived from urine sample of an individual in outpatient settings, and Paer4782MK was isolated from a blood culture of a patient with acute myeloid leukemia. Strains were sent to the National Reference Laboratory, department of Microbiology within the National Center of Infectious and Parasitic Diseases, Sofia, Bulgaria for carbapenem resistance confirmation purposes (Supplementary Table S1).

Phenotypic and molecular analysis

Strains were cultured on Columbia agar at 35 °C overnight. A single colony of each strain was identified via MALDI Biotyper (Bruker Daltonics GmbH & Co. KG, Bremen, Germany) with MALDI Reference 2022 Library v4.0.0. Antimicrobial Susceptibility Testing (AST) was performed using MICRONAUT-S Pseudomonas MIC and UMIC® Cefiderocol assay (Bruker Daltonics GmbH & Co. KG, Bremen, Germany). The interpretation of the AST results was in accordance to EUCAST clinical breakpoints v13.0.

Initially, the isolates were analyzed for carbapenemase activity by a modified CarbaNP test (Nordmann, Poirel and Dortet, 2012). In parallel, an in-house carbapenemase genes detection multiplex PCR was performed with the PCR components, conditions and protocols described in detail in Supplementary Table S1. Primer pairs for each gene were obtained from previously published sources, including *bla*$_{SIM}$, *bla*$_{SPM}$, *bla*$_{OXA-48-like}$, *bla*$_{GES}$ and *bla*$_{KPC}$ (Poirel, Naas and Nordmann, 2006; Mendes *et al.*, 2007; Cole *et al.*, 2009; Gröbner *et al.*, 2009) along with additional primer pairs for *bla*$_{IMP}$, *bla*$_{VIM}$ and *bla*$_{NDM}$ (Goudarzi *et al.*, 2019). High-resolution capillary electrophoresis was used following the PCR (QIAxcel, QIAGEN) with protocol 0M800 (3 kV for 800 s) for precise size estimation.

 doi:10.20944/preprints202307.2054.v1

Antimicrobial resistance gene expression assay of AMR-associated genes *mexA*, *mexC*, *mexE*, *mexX*, *ampC* and *oprD* was performed as previously described (Quale *et al.*, 2006; Wi *et al.*, 2018), and results interpreted according to (Cabot *et al.*, 2011). Biofilm formation was quantified by the crystal violet assay (Shukla and Rao, 2017).

Genomic and plasmid DNA extraction and WGS

Total genomic DNA extraction was performed with PureLink™ Genomic DNA Mini Kit (Invitrogen, Thermo Fisher Scientific Inc.) according to manufacturer's instructions except that all homogenization steps were carried out by pipetting. Plasmid DNA was acquired using NucleoSpin Plasmid Mini kit for plasmid DNA (Macherey-Nagel) following the "low-copy plasmid" protocol. Short-read NGS sequencing was performed using Illumina DNA Prep kit for sequencing libraries preparation and MiSeq V3 (2 × 300 bp), (Illumina, Inc., San Diego, CA, USA) for strains PA3541 and PA3796A, whereas PA4782 was sequenced on NextSeq 550 with V2.5 (2 x 150 bp) mid output flow cell. The same DNA extract without additional size-selection was used for long-read sequencing on a MinION Mk1C with the Rapid Barcoding Kit 96 (SQK-RBK110.96) and FLO-MIN106D (R9.4.1) (Oxford Nanopore Technologies plc.). The final purification step of the library pool was performed with 0.4x SPRI magnetic particles as recently suggested for removal of DNA fragments <1.5 kb (Alvarez-Arevalo *et al.*, 2022).

Cloning, transformation and conjugation/mating experiments

A 1150 bp fragment comprising the complete $bla_{\text{IMP-100}}$ (NG_203391.1) ORF, its promotor region and part of the *IntI* gene was cloned into pET28a T7pCONS TIR-2 sfGFP vector (cat. No 154464, Addgene, Inc., Watertown, MA 02472 USA) using the FastCloning protocol (Li *et al.*, 2011). The insert amplification and vector linearization PCR were described in detail in Supplementary table S2. A schematic representation of the cloning design is available in Supplementary Table S3. The PCR products mixed at 1:1 ratio were digested with *Dpn*I for 2 hours at 37°C.

Plasmid DNA from Paer4782MK strain was transformed into *P. aeruginosa* $PA01^{RifR}$. The transformation protocol for both the cloned IMP-100 and the whole Paer4782 plasmid preparation was identical (Tu *et al.*, 2016). Briefly, *E. coli* NEB-10 (New England Biolabs, UK) or *P. aeruginosa* $PA01^{RifR}$ recipients were incubated on Columbia agar at 35°C overnight. Few colonies were inoculated into 10 ml BHI broth and agitated at 200 rpm at 35°C until log phase (0.6 ± 0.05 OD) was achieved. Then, 1.4 ml suspension was aliquoted into 1.5 ml tubes and centrifuged at 8, 000 g for 2 min and the supernatant was discarded. Cell pellets were washed with 1 ml RT molecular grade water twice by gentle resuspension. Cell pellets were resuspended in 80 µl of RT molecular grade water. The digested vector and insert mix (20µl) or plasmid DNA were added, gently mixed, and immediately transferred into 2 mm gap electroporation cuvettes (VWR International, LLC). The electroporation was performed at 2500 mV on an Eporator® (Eppendorf). Immediately, 1 ml of BHI broth (RT) was added, gently mixed and incubated at 35°C for 2h. Fresh BHI agar plates containing 50 mg/L kanamycin and 8 mg/L ceftazidime were streaked with 50 µl of the transformants.

The spontaneous transferability of plasmids carrying resistance determinants was investigated by filter mating (Livermore and Jones, 1986) and combined mating technique (Walter, Porteous and Seidler, 1987). In attempt to increase the conjugation efficiency in *Pseudomonas* additional steps were implemented in the protocol as described in (Sakuda *et al.*, 2018). Rifampicin-resistant *E. coli* C600 and a spontaneous mutant of *P. aeruginosa* $PA01^{RifR}$ were used as recipient strains. Transconjugants were selectively cultured on MacConkey agar supplemented with ceftazidime (30 mg/L) and rifampicin (200 mg/L) (Sigma Chemical Co., St Louis, MO).

Bioinformatic analysis

Quality check of both long and short reads was performed with FastQC v0.11.9 (https://www.bioinformatics.babraham.ac.uk/projects/fastqc, accessed on 08.06.2023). Quality trimming and filtering of the raw reads was conducted with fastp v0.23.2 (Chen *et al.*, 2018) and

Preprints (www.preprints.org) | NOT PEER-REVIEWED | Posted: 31 July 2023 doi:10.20944/preprints202307.2054.v1

filtlong v0.2.1 (https://github.com/rrwick/Filtlong, accessed on 08.06.2023) for short and long reads, respectively. First, long-read-only assemblies were produced with Flye v0.2.1 (Kolmogorov *et al.*, 2019) and when no circular genome was achieved, hybrid assembly was attempted with Unicycler v0.4.8. The resulting assemblies were subsequently polished with tools such as Polypolish v0.5.0 (Wick and Holt, 2022), POLCA (Zimin and Salzberg, 2020) and MEDAKA v1.7.3 (ONT, https://github.com/nanoporetech/medaka, accessed on 15.06.2023). Assembly quality was assessed by multiple tools such as Quast v 5.0.2 (Mikheenko *et al.*, 2018), BUSCO v5.4.6 (Manni *et al.*, 2021) and CheckM v1.2.1 (Parks *et al.*, 2015). After genome quality evaluation, strain identification was performed with rMLST (Jolley *et al.*, 2012) and KmerFinder v 3.0.2 (Clausen, Aarestrup and Lund, 2018) with database version from 2022-07-11. Then, genomes were annotated with Bakta v 1.7 (Schwengers *et al.*, 2021) with database v5.0-full. Antibacterial resistance, phenotypic prediction and virulence determinants were identified with AMRFinderPlus v3.11.4 (Feldgarden *et al.*, 2021) and ResFinder v4.3.1 (Bortolaia *et al.*, 2020) with database version 2022-05-24 and VFanalyzer (database version from Jan 5 2023) (Liu *et al.*, 2022), respectively. Mob-suite v 3.1.4 (Robertson and Nash, 2018) was used for plasmid analysis. Analysis of ICEs was carried out with ICEfinder (Liu *et al.*, 2019). MLST profiles were inferred from sequence data using mlst v2.23.0 (Seemann T, mlst Github https://github.com/tseemann/mlst, accessed on 08.06.2023). *In-silico* serotyping was performed using PAst 1.0 (Thrane *et al.*, 2016). The functionality of the outer-membrane porin *oprD* was analyzed *in-silico* using the recently described PorinPredict tool (Biggel *et al.*, 2023).

Data availability

The complete genomes of the three strains were deposited in the European Nucleotide Archive (ENA) under project accession PRJEB62425. The genomes were assigned the following accession numbers: Paer4782MK - ERZ18545754, Paer3541 - ERZ18545673, Paer3796A - ERZ18545648. In the case of Paer4782MK, a novel variant of IMP-100, a subclass B1 metallo-beta-lactamase, was detected, validated and submitted to GenBank with accession number NG_203391.1.

Results

AMR and Biofilm formation

AST showed diverse resistance patterns among the tested strains. Paer4782MK exhibited high level of resistance to multiple classes of antibiotics, including all beta-lactams except aztreonam, aminoglycosides, and fluoroquinolones, consistent with an XDR phenotype. Paer3541 demonstrated resistance to cephalosporins and fluroquinolones but remained susceptible to carbapenems and aminoglycosides (except tobramycin). Paer3796A displayed resistance to all tested cephalosporins, carbapenems (except imipenem/relebactam), fluoroquinolones (except levofloxacin) and aminoglycosides (except amikacin). However, all three strains remained susceptible to colistin despite resistance to novel cephalosporin/inhibitor combinations like ceftazidime/avibactam and ceftolozane/tazobactam. Notably, both Paer4782MK and Paer3796A strains exhibited resistance to CFDC, a novel siderophore cephalosporin only recently approved for treatment of infections from MDR Gram-negatives (Syed, 2021). The AST profiles of the three IMP-carrying *P. aeruginosa* isolates are available in the Table 1.

Table 1. AST of IMP-carrying *P. aeruginosa* strains.

	MIC (µg/ml)					
Antimicrobials	**Paer4782**	**SIR**	**Paer3541**	**SIR**	**Paer3796A**	**SIR**
Piperacillin	≥32	R	16	I	8	I
Piperacillin/tazobactam	64/4	R	16/4	I	8/4	I
Cefepime	≥8	R	≥8	R	≥8	R
Ceftazidime	≥32	R	≥32	R	≥32	R
Ceftazidime/Avibactam	≥8/4	R	≥8/4	R	≥8/4	R

Preprints (www.preprints.org) | NOT PEER-REVIEWED | Posted: 31 July 2023 doi:10.20944/preprints202307.2054.v1

Ceftolozane/tazobactam	≥8/4	R	≥8/4	R	≥8/4	R
Cefiderocol	4	R	0.25	S	8	R
Imipenem	≥8	R	1	I	4	I
Imipenem/relebactam*	≥32/4	R	0.75/4	S	1.5/4	S
Meropenem	≥16	R	0.5	S	≥16	R
Meropenem/Vaborbactam*	≥256/8	R	0.5/8	S	≥256/8	R
Doripenem*	≥32	R	2	I	≥32	R
Aztreonam	4	I	8	I	≥16	R
Trimethoprim/sulfamethoxazole	≥8/152	n/a	≥8/152	n/a	≥8/152	n/a
Amikacin	≥32	R	16	S	4	S
Tobramycin	≥32	R	16	R	8	R
Gentamicin	16	n/a	≥32	n/a	≥32	n/a
Ciprofloxacin	≥8	R	≥8	R	2	R
Levofloxacin	≥8	R	≥8	R	2	I
Fosfomycin	32	n/a	≥128	n/a	<16	n/a
Colistin	<1	S	<1	S	<1	S

* - gradient strip; n/a - not applicable.

The modified CarbaNP test confirmed the presence of carbapenemases in all three isolates. Initially, the PCR results for *bla*$_{IMP}$ genes were negative. However, by employing alternative PCR primers (Goudarzi *et al.*, 2019) we successfully detected the presence of *bla*$_{IMP}$ in all three isolates and *bla*$_{VIM}$ in Paer4782MK.

We observed a positive correlation between the notable upregulation of the *mexXY* multi-drug efflux operon in Paer3541 and the elevated MICs for levofloxacin and ciprofloxacin, and also between low to moderate *mexXY* expression and lower fluoroquinolone MIC values in Paer3796A. Despite that Paer4782MK was characterized by moderate expression of the *mexCD* its association with the resistance profile remained uncertain as the strain already carried resistance genes for the majority of *mexCD* targets as seen from WGS results. Interestingly, all three strains exhibited negative expression of the outer membrane porin *oprD*. The gene expression levels are available in Supplementary Table S4. Lastly, all strains exhibited strong biofilm production.

Genome quality assessment and features

All three genomes achieved a completeness score close to 100%, indicating that the majority of the expected conserved genes were present. A high level of genome integrity without duplications is evidenced by the 99.2 % single-copy genes detected. No fragmented or missing conserved genes were identified. In line with these findings, CheckM revealed relatively low foreign DNA contamination levels ranging from 0.63% to 0.7%. Detailed information on assembly statistics and genome quality assessment are available in Supplementary Table S5.

Two plasmids p4782-IMP (61.5 Kbp) and p4782_002 (290.8 Kbp) were identified in Paer4782MK. p4782-IMP (OX638703.1) was related to the MOB$_F$ and MPF$_T$ plasmid pMOS94-like family. Notably, this plasmid carried the novel *bla*$_{IMP-100}$ (NG_203391.1) allele, in addition to other genes associated with AMR. The p4782_002 (OX638702.1), was untypable and lacked both resistance and virulence determinants, thus it was excluded from further analysis. The two plasmids detected in Paer3541 were p3541_1 (179.3 Kbp, OX638611.1) and p3541_2 (41.5 Kbp, OX638612.1). Similar to p4782-IMP, plasmid p3541_2 was MOB$_F$ and MPF$_T$ and was found to harbor a single *aac(6')-29* gene, encoding an aminoglycoside acetyltransferase. The plasmid p3541_1 had unknown MOB and MPF types, similar to p4782_002. For Paer3796A, a single plasmid p3796A (178.5 Kbp, OX638565.1) with unknown MOB and MPF types was identified and did not harbor any resistance or virulence determinants. Additional information regarding plasmid analysis is available in Supplementary Table S6.

Paer3541 and Paer3796A were assigned to ST621, a clone previously associated with *bla*$_{IMP}$ carriage (Giani *et al.*, 2018), while Paer4782MK belonged to the international high-risk clone ST233.

Preprints (www.preprints.org) | NOT PEER-REVIEWED | Posted: 31 July 2023 doi:10.20944/preprints202307.2054.v1

In-silico serotyping revealed that Paer3541 and Paer3796A were serogroup O4, while Paer4782MK was O11.

Detection of AMR determinants

The AMR screening uncovered a diverse array of genes (Figure 1.) All three isolates demonstrated the presence of an IMP carbapenemase, with the unique *bla*IMP-100 allele identified in a pMOS94-like plasmid in Paer4782MK. Additionally, strain Paer4782MK also harbored *bla*VIM-4. Two other closely related chromosomal *bla*IMP variants, IMP-13 and IMP-84, were detected in Paer3541 and Paer3796A respectively. Additional acquired ESBL such as PER-1 and multiple genetic determinants associated with resistance to most non-beta-lactam antimicrobial groups were present as well.

In-silico analysis of the *oprD* gene revealed that both Paer3541 and Paer3796A harbour an intact and functional *oprD* porin. Despite the identification of a missense mutation (S325F) in the *oprD* gene of Paer3796A, the gene appeared intact. Conversely, a truncated *oprD* protein was evident in Paer4782MK potentially compromising its function (Supplementary Table S6). No known mutations related to efflux overexpression were detected.

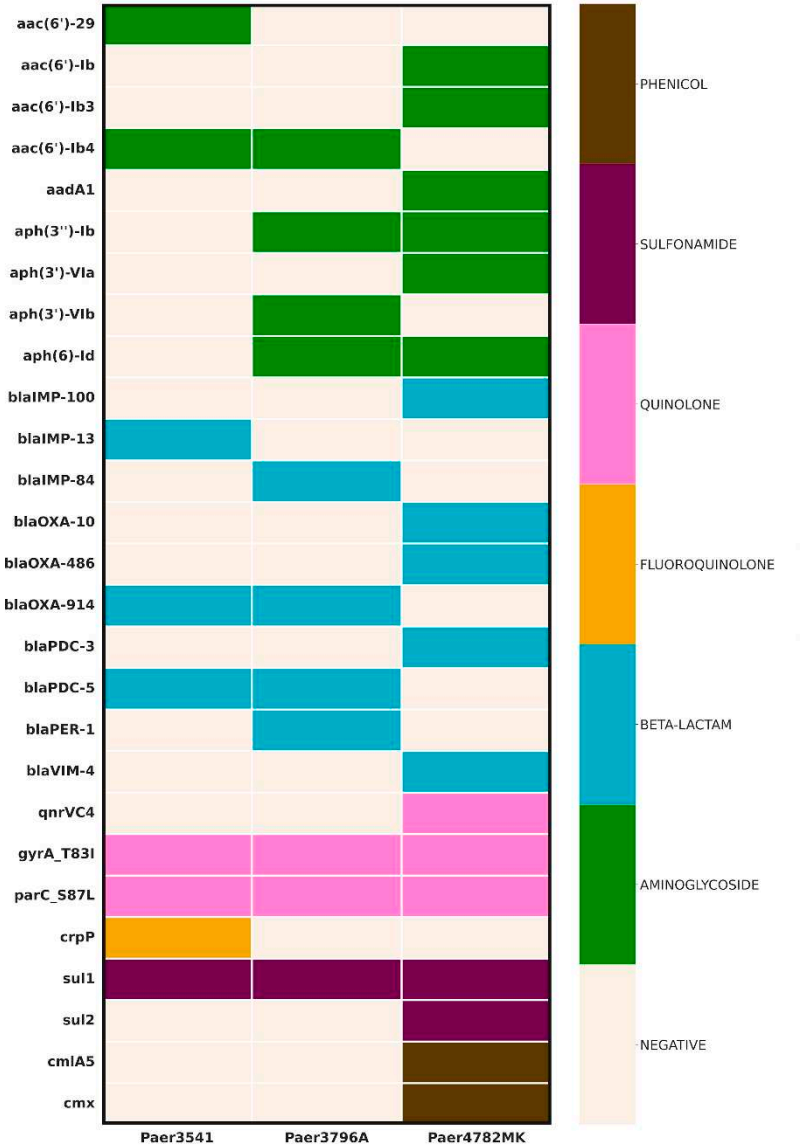

Figure 1. Genomic inference of resistance determinants. Columns represent strains, whereas AMR genes are in rows.

Preprints (www.preprints.org) | NOT PEER-REVIEWED | Posted: 31 July 2023 doi:10.20944/preprints202307.2054.v1

Detection of virulence determinants

All three isolates exhibited virulence factors related to adherence and motility, including flagella, type IV pili biosynthesis, and twitching motility. Alginate biosynthesis genes known for promoting bacterial resilience against harsh conditions and host immune responses (Franklin *et al.*, 2011) were detected in all isolates. However, certain antimicrobial-related factors (*phzC2*, *phzD2*, *phzE2*, *phzF2*, and *phzG2*) were absent compared to the reference strain PA01. Phospholipases C and D were identified, including *plcH*, known for its hemolytic activity (Vasil *et al.*, 2009). Siderophore production genes were present in Paer3541 and Paer3796A, while the *pvdD* gene, responsible for pyoverdine production, was lacking in Paer4782MK, indicating impaired pyoverdine synthesis (Meldrum, no date). Additional virulence factors, including alkaline protease (AprA), elastase (LasA and LasB), Protease IV (PrpL), and exotoxin A (ToxA) were also detected. Quorum sensing components such as acylhomoserine lactone synthase (HdtS), transcription factors (LasI, RhlI), receptors (LasR, RhlR), as well as the GacS/GacA two-component system and type VI secretion system (H-T6SS) components were found in all three isolates. Rhamnolipid biosynthesis genes (*rhlA*, *rhlB*, and *rhlC*), associated with host cell infiltration and biofilm formation (McClure and Schiller, 1996; Zulianello *et al.*, 2006) were identified. The isolates exhibited T3SS effectors, including *exoS*, *exoT*, and *exoY*, involved in manipulating host cell signaling pathways and immune responses, along with T3SS genes such as *pcrV*, *popB*, *popD*, and *pscF*, indicating the presence of a functional T3SS machinery capable of delivering effector molecules into host cells. The isolates harboured genes associated with hydrogen cyanide production (HcnA, HcnB, and HcnC), a potent toxic compound known to disrupt cellular processes and impact aerobic respiration (Ryall *et al.*, 2008). Furthermore, the MDR plasmid p4782-IMP in Paer4782MK harbored the *katG* gene, which is involved in oxidative stress protection (Manca *et al.*, 1999). A summary of the virulence screening results can be found in Supplementary Table S7.

Plasmid analysis

The complete sequence of plasmid p4782-IMP was subjected to a BLAST search against the nr/nt database of NCBI, and a neighbor-joining tree was constructed with the most similar plasmids (n=19). Interestingly, plasmid p3541_2 was identified as closely related to p3782-IMP. Additionally, all plasmids were screened for AMR genes and the results were illustrated as a heatmap and linked to the phylogenetic tree (Figure 2.).

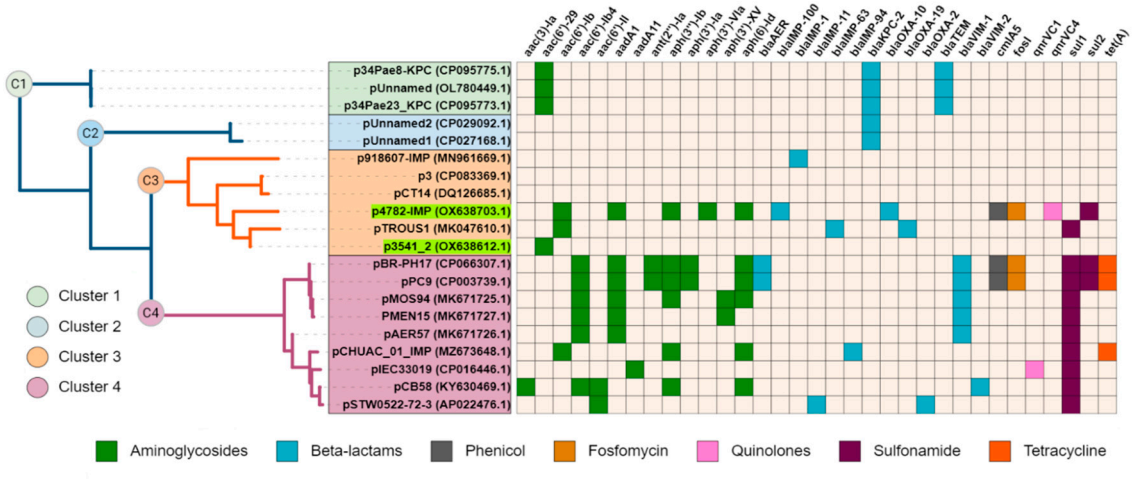

Figure 2. Phylogenetic tree and resistance heatmap. Plasmids from the current study are highlighted in green. The different tree clusters (C1 ÷ C4) are distinguished by varying colors. The heatmap legend below provides information on the antibiotic class of the detected genes. The tree was generated with neighbor-joining after NCBI blast with Max Seq Difference score ≥ 0.75. The heatmap and the tree were visualized with iToL 6.8 (https://itol.embl.de/about.cgi, accessed on 25.07.2023).

Preprints (www.preprints.org) | NOT PEER-REVIEWED | Posted: 31 July 2023 doi:10.20944/preprints202307.2054.v1

Upon observation, cluster C1 was found to encompass three plasmids with unknown MOB type that encoded KPC enzymes. The remaining clusters C2-C4 comprised plasmids from the MOB_F and MPF_T families. C2 was similar to C3 plasmids, but unlike them carried only KPC enzyme. C3 and C4 both exhibited relatedness to the pMOS94-like plasmids (Pilato *et al.*, 2019a). Interestingly, C3 plasmids had lower density of AMR-associated genes compared to C4. Despite the high abundance of AMR genes found on plasmid p4782-IMP similar to C4 plasmids, it was grouped within the lower-resistance cluster C3.

Additionally, an in-depth comparison was conducted between the most phylogenetically related carbapenemase-harboring plasmids and p4782-IMP using the Gview server's BLAST Atlas. The analysis unveiled a distinctive transposon insertion within the MOB_F/MPF_T family plasmid backbone, as illustrated in Figure 3. This novel transposon carried the novel *bla*$_{IMP-100}$ allele, as well as multiple AMR determinants, which accounted for the atypical abundance of resistance genes observed in p4782-IMP.

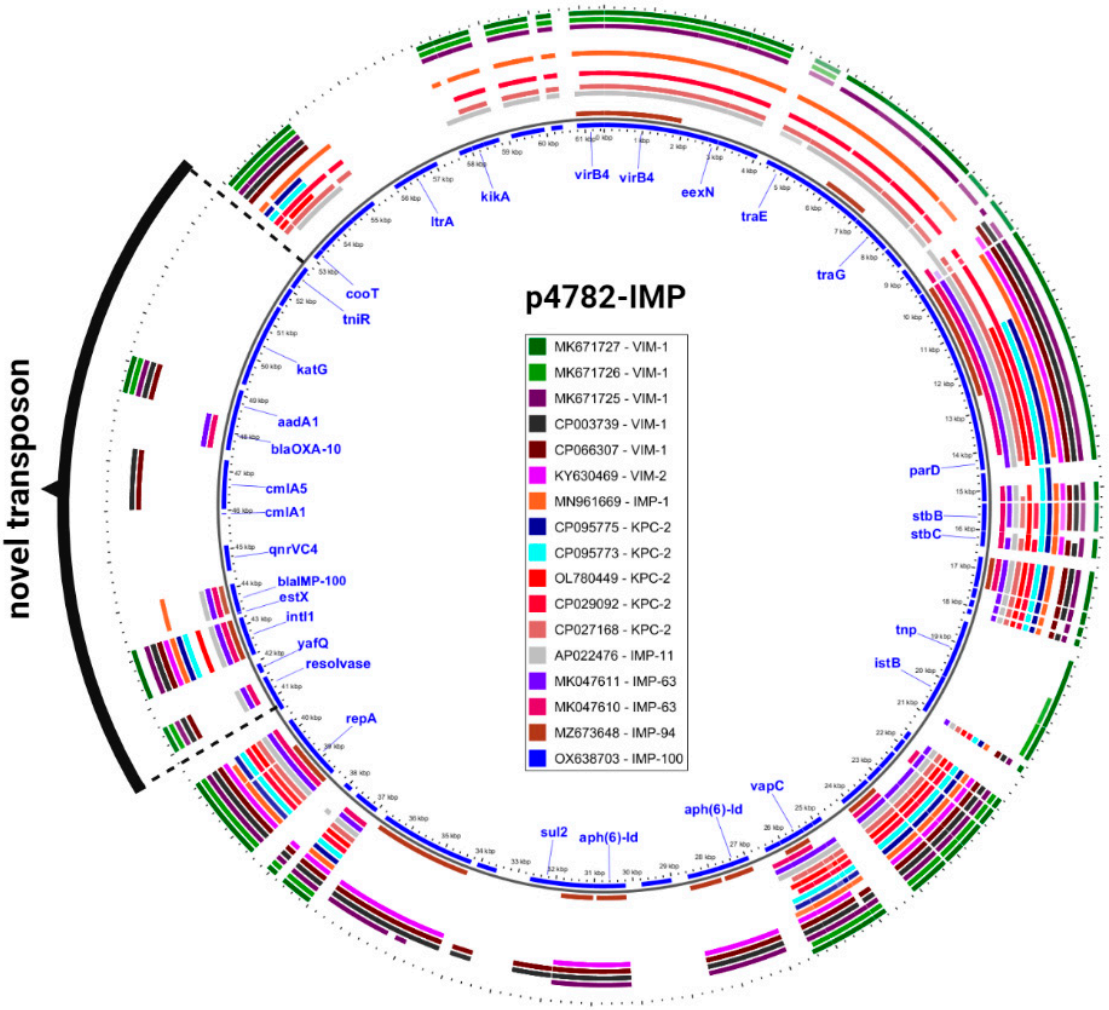

Figure 3. Closest plasmids with carbapenemases. The plasmid accession numbers are listed in the legend and colored differently. The most inner circle (blue) is p4782-IMP suits as a reference for comparison. Only important gene annotations were visualized in blue text. The novel transposon is shown in black. The figure was produced with Gview Atlas server (https://server.gview.ca, accessed on 25.07.2023).

Cloning, Transformation and Conjugation

Transformants (PA01-p4782-IMP and *E. coli* NEB10-IMP-100) were successfully obtained. AST was conducted on both the recipients ($PA01^{RifR}$ and *E. coli* NEB10) and the transformants. The results

Preprints (www.preprints.org) | NOT PEER-REVIEWED | Posted: 31 July 2023 doi:10.20944/preprints202307.2054.v1

are provided in Table 2. Firstly, the introduction of the whole p4782-IMP into PAO1 increased the MIC for imipenem at least 8 fold, and for meropenem at least 128 fold. In comparison, IMP-100 gene alone in *E. coli* NEB10-IMP-100 increased the MIC for imipenem at least 2 fold, and for meropenem at least 16 fold. Although *in-silico* analysis with mob-suite suggested the transferability of the MDR plasmid, all mating experiments were unsuccessful for both *E. coli* NEB10 and PA01 despite the numerous attempts and variations.

Table 2. AST of *P. aeruginosa* and *E. coli* transformants.

	MIC (μg/ml) for strain				
	Donor Strain *Pseudomonas aeruginosa*			*Escherichia coli*	
Antimicrobials	**Paer4782**	**PA01**	**PA01-p4782-IMP**	**E.coli NEB10**	**E.coli NEB10-IMP-100**
Piperacillin	≥32	<4	≥32	<4	4
Piperacillin/Tazobactam	64/4	1/4	64/4	<1/4	4/4
Cefepime	≥8	<1	≥8	<1	≥8
Ceftazidime	≥32	0.5	≥32	<0.25	≥32
Ceftazidime/Avibactam	≥8/4	<1/4	≥8/4	<1/4	≥8/4
Ceftolozane/Tazobactam	≥8/4	<1/4	≥8/4	<1/4	≥8/4
Cefiderocol	4	0.25	8	0.125	0.125
Imipenem	≥8	<1	≥8	<1	2
Imipenem/Relebactam*	≥32/4	0.25/4	8/4	0.125/4	2/4
Meropenem	≥16	<0.125	≥16	<0.125	2
Meropenem/Vaborbactam*	≥256/8	0.25/8	48/8	≤0.016/8	2/8
Doripenem*	≥32	0.1	≥32	0.08	6
Ertapenem*	n/a	n/a	n/a	0.023	6
Aztreonam	4	1	8	<1	<1
Trimethoprim/Sulfamethoxazole	≥8/152	1/19	1/19	<1/19	<1/19
Amikacin	≥32	<4	4	<4	<4
Tobramycin	≥32	<0.25	8	<0.25	0.5
Gentamicin	16	0.25	16	0.25	0.25
Ciprofloxacin	≥8	0.0625	1	<0.06	0.06
Levofloxacin	≥8	0.125	1	<0.125	<0.125
Fosfomycin	32	16	≥128	<16	<16
Colistin	<1	<1	<1	<1	<1

* - gradient strip; n/a - not applicable

Phylogeny and Genetic environment of blaIMP-100 in Paer4782MK

A phylogenetic analysis of all IMP variants was conducted through protein sequence alignment and subsequent construction of a phylogenetic tree (Figure 4). The clustering of IMP alleles and the labeling of the resulting groups was completed according to a clustering scheme suggested previously (Li *et al.*, 2023), thus maintaining consistency. The novel allele IMP-100 falls into the G6 cluster revealing closest similarity to IMP-63, IMP-12 and IMP-90. The *bla*$_{\text{IMP-100}}$ gene was positioned as the first cassette under weak PcW+P2 promotor (Wei *et al.*, 2011) in a novel *In1300-like Tn402* type integron platform and followed by *qnrVC4*, *cmlA5*, and *bla*$_{\text{OXA-10}}$ cassettes (Figure 5).

Preprints (www.preprints.org) | NOT PEER-REVIEWED | Posted: 31 July 2023 doi:10.20944/preprints202307.2054.v1

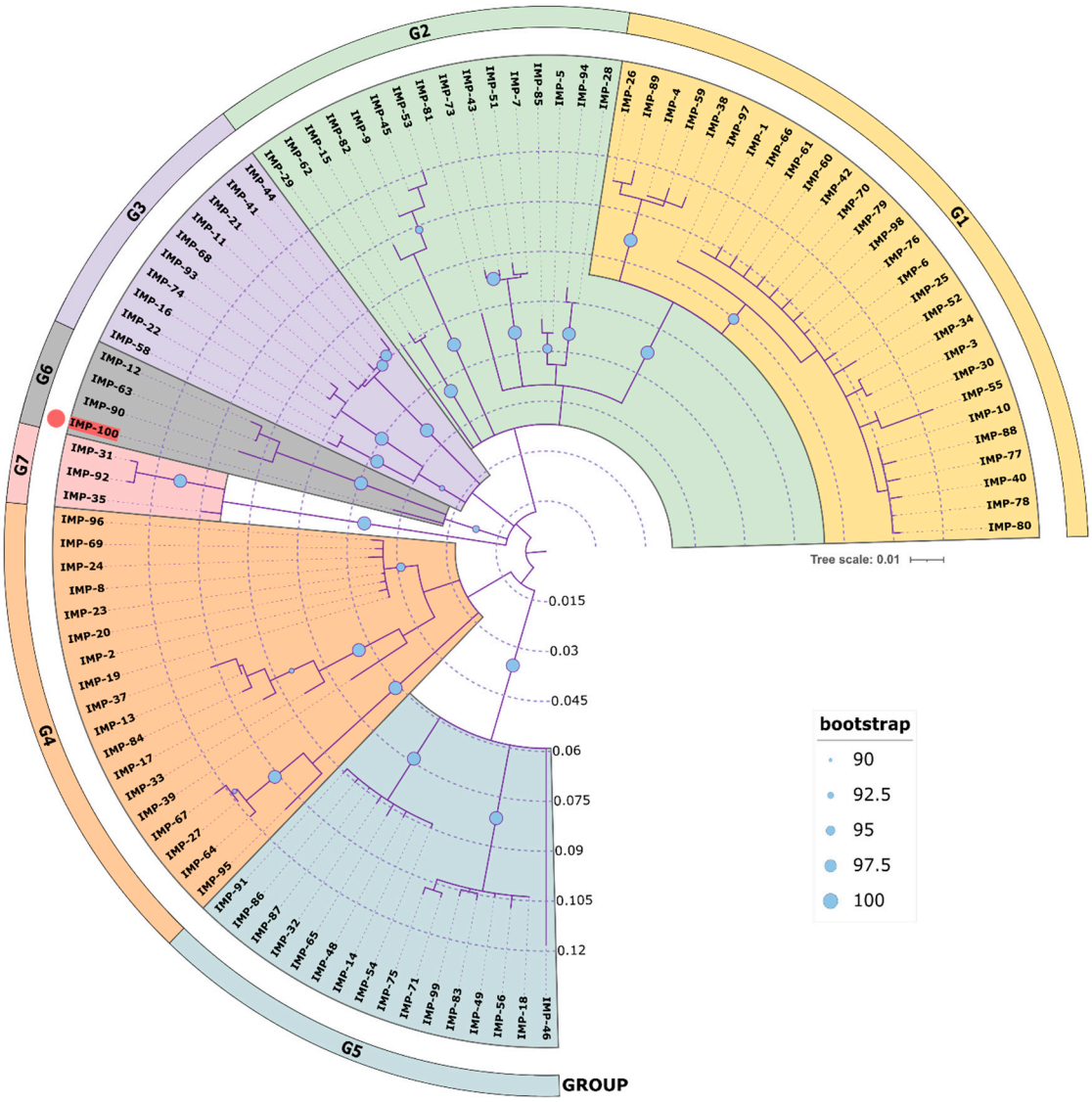

Figure 4. Phylogenetic tree of all available IMP variants. All NCBI available protein sequences were download and aligned with *Muscle* alignment 3.8.425 in Geneious Prime 2022 and phylogenetic tree was constructed with Geneious Tree builder with Jukes-Cantor genetic distance model and neighbor-joining build method with bootstrap 1000. The tree was visualized in iToL 6.8 (https://itol.embl.de/about.cgi, accessed on 25.07.2023). Cluster groups G1 ÷ G7 were colored differently in accordance to Xinyue et al. and the new IMP-100 alelle is colored in red with red dot at the tip of the leaf. Bootstrap indices are represented as circles placed at each node ranging in size from 90 (small circle) to 100 (large circle) to show the degree of cluster consistency.

Similar cassette array (*In1300*) was previously reported in *Aeromonas salmonicida* MDR plasmid pS121-1a (CP022170). The p4782-IMP integron was preceded by a novel putative IS, hereby referred to as *IS4782* flanked by imperfect 25bp inverted repeats IRL (TGTCATTTTCAGAAG**G**CGACTGCAC) and IRR (TGTCATTTTCAGAAG**A**CGACTGCAC) closely resembling those of *ISPa17* and *Tn402*. IRR was also found on the far 3′ end of the *Tn402* integron as well (Figure 4). The *IS4782* harbored three genes: the *yafQ* toxin gene, putative resolvase (188AA) and short transposase (128AA). This putative IS was lacking any significant homologues within the ISFinder or TnCentral databases (Siguier *et al.*, 2006; Ross *et al.*, 2021). BLAST search was able to find eight identical hits (all plasmid borne and one being p3541_2 plasmid reported here) only matching the resolvase and transposase genes and not the whole IS. It was hypothesized that this element is capable of horizontal dissemination either alone or with the *Tn402* integron due to sharing the same

Preprints (www.preprints.org) | NOT PEER-REVIEWED | Posted: 31 July 2023 doi:10.20944/preprints202307.2054.v1

inverted repeats. Next, we managed to identify and map related mobile elements in order to detect a hypothetical origin of the novel transposon (Figure 5). The 5′ end most closely resembled the tnp/resolvase combination found in a *P.aeruginosa* transposon from the Czech Republic (KY860572) (Papagiannitsis *et al.*, 2017) followed by an integron carrying the IMP-100 that was highly similar to the one from *Aeromonas salmonicida* MDR plasmid pS121-1a (Figure 5). The 3′ end of the transposon resembled a remnant from another one found in *Enterobacter cloaceae* plasmid (AP022231) containing the *katG*, *dps* and the *tniR*. Similar structures have been reported in most pMOS94-like plasmids where *ISPa17* preceded carbapenemase carrying *Tn402* integrons (Pilato *et al.*, 2019a). Recently it was hypothesized that the *ISPa17* transposase might be capable of mobilization of adjacent *Tn402* integrons resulting in distinct transposon elements (Papa-Ezdra *et al.*, 2023). The IMP-100 transposon had 5bp direct repeats (AAAAC) located up to 26bp apart from each IR, which although unexpected might be suggestive of past transposition events. Finally, we also discovered a probable ancestral insertion site of the whole IS4782-*Tn402* structure located in a *P. putida* plasmid from Brazil (CP016446) (Souza *et al.*, 2023).

For the remaining two strains we found that IMP-13 (Paer3541) and IMP-84 (Paer3796) were located chromosomally in class I integrons embedded in *Tn5051-like* transposons, whereas VIM-4 (in Paer4782) was found in *In237-like* integron. Importantly, all these MBLs were components of self-transmissible T4SS-type ICEs meaning they are capable of dissemination by horizontal gene transfer (Supplemental Fig S8). Lastly, all putative novel mobile genetic elements were submitted to the respective databases (ISFinder, TnRegistry and INTEGRALL) (Siguier *et al.*, 2006; Moura *et al.*, 2009; Tansirichaiya, Rahman and Roberts, 2019).

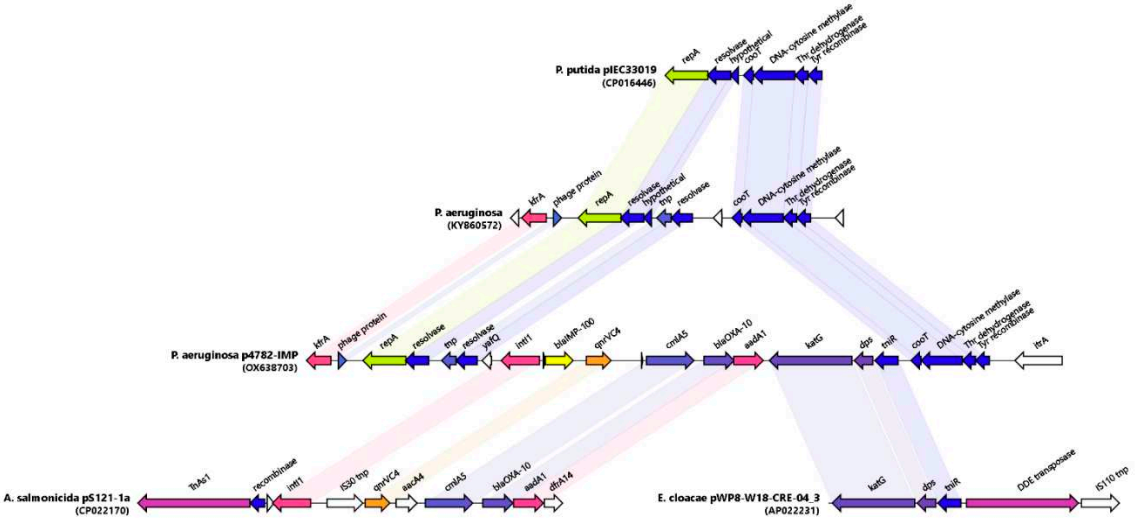

Figure 5. Genetic environment of *bla*IMP-100. A hypothesized origin of the novel transposon *IS4782* is depicted. Matching genes from the different sources are connected and identically colored. Non-matching genes (either hypothetical proteins or not) are shown in white. Unlabeled genes are hypothetical. The figure was created with Clinker v0.0.28 (https://github.com/gamcil/clinker, accessed on 25.07.2023).

Discussion

Between 2018 and 2022, three epidemiologically unrelated MDR *P. aeruginosa* strains were obtained from diverse clinical sources. Surprisingly, the modified CarbaNP test and the PCR for carbapenemase detection yielded conflicting results for strains Paer3541 and Paer3796A with PCR being negative. Furthermore, WGS analysis revealed the presence of *bla*IMP-13 in Paer3541 and *bla*IMP-84 in Paer3796A. These findings were suggestive that the primers used to target *bla*IMP genes were ineffective and had to be replaced. Paer4782MK was the most recent isolate of the three and the *bla*IMP was therefore successfully detected with the updated PCR assay (Goudarzi *et al.*, 2019). It is important to note that the availability of several alternative methods for carbapenemase detection may prove

useful as well as regular updates of the methodologies are required to correctly detect the presence of rare gene variants.

Among the carbapenemases detected in Bulgaria, VIM-type enzymes are frequently observed (Schneider *et al.*, 2008; Strateva, Setchanova and Peykov, 2021), but occurrence of NDM-1, GES-5, and OXA-50 carbapenemases were also documented (Petrova *et al.*, 2019; Kostyanev *et al.*, 2020). To our knowledge, this study represents the first report of *bla*$_{IMP}$ detection in three clinical MDR isolates from Bulgaria. Additionally, we identified a novel allele of the *bla*$_{IMP}$ gene, designated *bla*$_{IMP-100}$, located on a MDR plasmid (p4782-IMP) within Paer4782MK. This strain also carried a chromosomally-encoded *bla*$_{VIM-4}$ carbapenemase and was categorized as ST233, a globally prevalent multidrug-resistant clone (Aguilar-Rodea *et al.*, 2017), often associated with *bla*$_{VIM-2}$ production (del Barrio-Tofiño, López-Causapé and Oliver, 2020). Paer3541 (IMP-13) and Paer3796A (IMP-84) were classified as ST621, an epidemic clone known for its association with *bla*$_{IMP}$ production and a higher prevalence of *pldA*, a trans-kingdom phospholipase T6SS effector (Boulant *et al.*, 2018). This effector is associated with the H2 Type VI secretion system (H2-T6SS) and involved in bacterial endocytosis (Russell *et al.*, 2013).

In line with previous research demonstrating a correlation between ST233 and the *exoS*+ (*exoU*-) genotype (del Barrio-Tofiño, López-Causapé and Oliver, 2020), our virulence analysis revealed that Paer4782MK (ST233) exhibited this specific genotype. ExoU and ExoS are mutually exclusive T3SS effectors, with ExoS leading to delayed apoptotic cell death, while ExoU induces rapid host cell lysis (Hauser, 2009). Regarding serotypes, our findings align with existing literature (Recio *et al.*, 2020), demonstrating a strong association between serotypes O4 and O11 and MDR phenotypes. Typically, the O4 serotype is associated with the *exoU*-negative genotype, while the O11 serotype is linked to the *exoU*-positive genotype. Interestingly, Paer4782MK tested negative for *exoU* and exhibited the *exoS* genotype. Furthermore, despite recent studies suggesting an association between ST233 and serotype O6 (Pottier *et al.*, 2023), our classification of Paer4782MK as ST233:O11 deviates from this anticipated relationship.

Upon analyzing the WGS data, it was determined that the observed negative expression of *oprD* in the expression assay was due to an identical 10 amino acid indel, which prevented primer binding across all three isolates, thereby rendering the results invalid. Additionally, PorinPredict tool confirmed the presence of an intact and functional *oprD* porin in Paer3541, which likely contributed to its susceptibility to and lowest MIC values of meropenem, imipenem, meropenem/vaborbactam, and imipenem/relebactam of all three strains. Despite the occurrence of a missense mutation S325F, the *oprD* integrity in Paer3796A remained unaffected. In fact, the presence of this mutation has been associated in a potential increase in the MIC of imipenem (Khoury *et al.*, 2019). However, further investigations are necessary to determine its precise impact. Lastly, both our observation and PorinPredict concluded that the *oprD* gene in Paer4782MK is truncated, therefore its functionality was compromised, consistent with the higher reported MIC values for meropenem, imipenem, meropenem/vaborbactam, and imipenem/relebactam in this particular strain.

Phylogenetic analysis demonstrated a close genetic association between the plasmid p4782-IMP, harboring the novel *bla*$_{IMP-100}$ allele, and the pMOS94-like plasmid family. The pMOS94 plasmid family was recently recognized as an emerging lineage involved in dissemination of MBL genes among *Pseudomonas* species, also commonly carry *bla*$_{VIM}$ and *bla*$_{IMP}$ genes, and recently *bla*$_{BIM}$, and some of them were found to display disruptions in the transfer module (*trw*), thus impeding conjugation (Pilato *et al.*, 2019b). In the genetic environment of the *trw* transfer module of p4782-IMP we could not identify any disruption, so the observed unsuccessful mating experiments could be due to other reasons. Next, the comparison with the nearest carbapenemase-harboring plasmids revealed an insertion of unique transposon in p4782-IMP, carrying multiple AMR determinants. The transformation of PA01 with the p4782-IMP plasmid resulted in a resistance profile similar to that of the Paer4782MK strain, demonstrating the impact of p4782-IMP in reducing susceptibility to important antibiotic classes and conferring multiple drug resistance. Furthermore, the transfer of the entire plasmid into the PA01 conferred resistance to CFDC. On the other hand, in the case of the *E. coli* NEB10 transformant carrying only the *bla*$_{IMP-100}$ gene, there was no significant increase in the CFDC

MIC suggesting that the CFDC resistance was a result of complex interplay between multiple genes present on the plasmid, in addition to *bla*IMP-100.

Conclusion

Our study is the first to our knowledge to document the *bla*IMP in clinical *P. aeruginosa* from Bulgaria. We also discovered a novel *bla*IMP-100 allele located on a MDR plasmid (p4782-IMP). The plasmid in turn conferred resistance to multiple antibiotics including CFDC, as shown by the similar MDR pattern revealed in PA01 transformant. However, by examining transformants carrying only the *bla*IMP-100 gene, we observed that CFDC MIC values did not show a substantial increase, further implying the involvement of other plasmid genes in the development of resistance to this novel agent. Lastly, our study emphasizes the importance of employing multiple methods for carbapenemase screening, given that conventional methods, apart from WGS, might show reduced sensitivity and neglect carbapenemase activity or genes.

Supplementary Materials: The following supporting information can be downloaded at the website of this paper posted on Preprints.org., S1. Carba mPCR; S2. Cloning protocol template; S3. Clonning schematic; S4. Expression analysis; S5. Genome Quality; S6. MOB Suite results; S7. oprD analysis; S8. Virulence factors; S9. ICEs.

Author Contributions: All authors contributed in different aspects. Conceptualization, methodology and validation - I. I., R.H., S.S. and I.S. Software, formal analysis, investigation – I.S., D.D., I.I., D.T., E.D.; resources S.S, E.D, R.H, data curation – D.D., D.T., S.S.; writing—original draft preparation – I.S., I.I., D.D., writing—review and editing – I.S., I.I., S.S., D.T., E.D., visualization – D.D., I.S., supervision, project administration, funding acquisition – I.I.All authors have read and agreed to the published version of the manuscript.

Funding: This study was supported by The Bulgarian National Science Fund under Grant КП-06-H23/5 and the European Regional Development Fund through the Operational Program Science and Education for Smart Growth 2014–2020; Grant BG05M2OP001-1.002-0001-C04 "Fundamental Translational and Clinical Research in Infection and Immunity".

Data Availability Statement: All used data is included in the main text and in the supplementary materials. Relevant links and/or references to other sources are included in the main text. The generated information and/or datasets analyzed during the current study are available from the corresponding author on reasonable request.

Conflicts of Interest: The authors declare no conflict of interest. The funders had no role in the design of the study; in the collection, analyses, or interpretation of data; in the writing of the manuscript; or in the decision to publish the results.

This study was partially reported as a poster M193 at the 10th FEMS Congress of European Microbiologists, 9-13 June 2023, Hamburg, Germany

References

1. Aguilar-Rodea, P. et al. (2017) 'Identification of extensive drug resistant Pseudomonas aeruginosa strains: New clone ST1725 and high-risk clone ST233', PLoS ONE, 12(3). Available at: https://doi.org/10.1371/JOURNAL.PONE.0172882.
2. Alvarez-Arevalo, M. et al. (2022) 'Extraction and Oxford Nanopore sequencing of genomic DNA from filamentous Actinobacteria', STAR protocols, 4(1). Available at: https://doi.org/10.1016/J.XPRO.2022.101955.
3. del Barrio-Tofiño, E., López-Causapé, C. and Oliver, A. (2020) 'Pseudomonas aeruginosa epidemic high-risk clones and their association with horizontally-acquired β-lactamases: 2020 update', International Journal of Antimicrobial Agents, 56(6), p. 106196. Available at: https://doi.org/10.1016/J.IJANTIMICAG.2020.106196.
4. Biggel, M. et al. (2023) 'PorinPredict: In Silico Identification of OprD Loss from WGS Data for Improved Genotype-Phenotype Predictions of P. aeruginosa Carbapenem Resistance', Microbiology spectrum, 11(2). Available at: https://doi.org/10.1128/SPECTRUM.03588-22.
5. Bortolaia, V. et al. (2020) 'ResFinder 4.0 for predictions of phenotypes from genotypes', Journal of Antimicrobial Chemotherapy, 75(12), pp. 3491–3500. Available at: https://doi.org/10.1093/JAC/DKAA345.
6. Boulant, T. et al. (2018) 'Higher Prevalence of PldA, a Pseudomonas aeruginosa Trans-Kingdom H2-Type VI Secretion System Effector, in Clinical Isolates Responsible for Acute Infections and in Multidrug Resistant Strains', Frontiers in Microbiology, 9. Available at: https://doi.org/10.3389/FMICB.2018.02578.

7. Cabot, G. et al. (2011) 'Overexpression of AmpC and Efflux Pumps in Pseudomonas aeruginosa Isolates from Bloodstream Infections: Prevalence and Impact on Resistance in a Spanish Multicenter Study', Antimicrobial Agents and Chemotherapy, 55(5), p. 1906. Available at: https://doi.org/10.1128/AAC.01645-10.
8. Chen, S. et al. (2018) 'fastp: an ultra-fast all-in-one FASTQ preprocessor', Bioinformatics, 34(17), pp. i884–i890. Available at: https://doi.org/10.1093/BIOINFORMATICS/BTY560.
9. Clausen, P.T.L.C., Aarestrup, F.M. and Lund, O. (2018) 'Rapid and precise alignment of raw reads against redundant databases with KMA', BMC Bioinformatics, 19(1), pp. 1–8. Available at: https://doi.org/10.1186/S12859-018-2336-6/TABLES/2.
10. Cole, J.M. et al. (2009) 'Development and Evaluation of a Real-Time PCR Assay for Detection of Klebsiella pneumoniae Carbapenemase Genes', Journal of Clinical Microbiology, 47(2), p. 322. Available at: https://doi.org/10.1128/JCM.01550-08.
11. Daikos, G.L. et al. (2021) 'Review of Ceftazidime-Avibactam for the Treatment of Infections Caused by Pseudomonas aeruginosa', Antibiotics, 10(9). Available at: https://doi.org/10.3390/ANTIBIOTICS10091126.
12. Feldgarden, M. et al. (2021) 'AMRFinderPlus and the Reference Gene Catalog facilitate examination of the genomic links among antimicrobial resistance, stress response, and virulence', Scientific Reports 2021 11:1, 11(1), pp. 1–9. Available at: https://doi.org/10.1038/s41598-021-91456-0.
13. Franklin, M.J. et al. (2011) 'Biosynthesis of the Pseudomonas aeruginosa Extracellular Polysaccharides, Alginate, Pel, and Psl', Frontiers in microbiology, 2(AUG). Available at: https://doi.org/10.3389/FMICB.2011.00167.
14. Giani, T. et al. (2018) 'Italian nationwide survey on Pseudomonas aeruginosa from invasive infections: activity of ceftolozane/tazobactam and comparators, and molecular epidemiology of carbapenemase producers', Journal of Antimicrobial Chemotherapy, 73(3), pp. 664–671. Available at: https://doi.org/10.1093/JAC/DKX453.
15. Goudarzi, H. et al. (2019) 'Rapid detection and molecular survey of blaVIM, blaIMP and blaNDM genes among clinical isolates of Acinetobacter baumannii using new multiplex real-time PCR and melting curve analysis', BMC Microbiology, 19(1). Available at: https://doi.org/10.1186/S12866-019-1510-Y.
16. Gröbner, S. et al. (2009) 'Emergence of carbapenem-non-susceptible extended-spectrum β-lactamase-producing Klebsiella pneumoniae isolates at the university hospital of Tübingen, Germany', Journal of Medical Microbiology, 58(7), pp. 912–922. Available at: https://doi.org/10.1099/JMM.0.005850-0/CITE/REFWORKS.
17. Gupta, V. (2008) 'Metallo beta lactamases in Pseudomonas aeruginosa and Acinetobacter species', http://dx.doi.org/10.1517/13543784.17.2.131, 17(2), pp. 131–143. Available at: https://doi.org/10.1517/13543784.17.2.131.
18. Hauser, A.R. (2009) 'The Type III Secretion System of Pseudomonas aeruginosa: Infection by Injection', Nature reviews. Microbiology, 7(9), p. 654. Available at: https://doi.org/10.1038/NRMICRO2199.
19. Hong, D.J. et al. (2015) 'Epidemiology and Characteristics of Metallo-β-Lactamase-Producing Pseudomonas aeruginosa', Infection & Chemotherapy, 47(2), p. 81. Available at: https://doi.org/10.3947/IC.2015.47.2.81.
20. Jolley, K.A. et al. (2012) 'Ribosomal multilocus sequence typing: universal characterization of bacteria from domain to strain', Microbiology (Reading, England), 158(Pt 4), pp. 1005–1015. Available at: https://doi.org/10.1099/MIC.0.055459-0.
21. Khoury, J.Y. El et al. (2019) 'Chemogenomic Screen for Imipenem Resistance in Gram-Negative Bacteria', mSystems, 4(6). Available at: https://doi.org/10.1128/MSYSTEMS.00465-19.
22. Kolmogorov, M. et al. (2019) 'Assembly of long, error-prone reads using repeat graphs', Nature Biotechnology 2019 37:5, 37(5), pp. 540–546. Available at: https://doi.org/10.1038/s41587-019-0072-8.
23. Kostyanev, T. et al. (2020) 'Emergence of ST654 Pseudomonas aeruginosa co-harbouring blaNDM-1 and blaGES-5 in novel class I integron In1884 from Bulgaria', Journal of Global Antimicrobial Resistance, 22, pp. 672–673. Available at: https://doi.org/10.1016/J.JGAR.2020.06.008.
24. Li, C. et al. (2011) 'FastCloning: A highly simplified, purification-free, sequence- and ligation-independent PCR cloning method', BMC Biotechnology, 11(1), pp. 1–10. Available at: https://doi.org/10.1186/1472-6750-11-92/FIGURES/6.
25. Li, X. et al. (2023) 'Characterization of Three Novel IMP Metallo-β-Lactamases, IMP-89, IMP-91, and IMP-96, and Diverse blaIMP-Carrying Accessory Genetic Elements from Chinese Clinical Isolates', Microbiology spectrum, 11(3). Available at: https://doi.org/10.1128/SPECTRUM.04986-22.
26. Liu, B. et al. (2022) 'VFDB 2022: a general classification scheme for bacterial virulence factors', Nucleic acids research, 50(D1), pp. D912–D917. Available at: https://doi.org/10.1093/NAR/GKAB1107.
27. Liu, M. et al. (2019) 'ICEberg 2.0: an updated database of bacterial integrative and conjugative elements', Nucleic Acids Research, 47(D1), pp. D660–D665. Available at: https://doi.org/10.1093/NAR/GKY1123.

28. Livermore, D.M. and Jones, C.S. (1986) 'Characterization of NPS-1, a novel plasmid-mediated β-lactamase, from two Pseudomonas aeruginosa isolates', Antimicrobial Agents and Chemotherapy, 29(1), pp. 99–103. Available at: https://doi.org/10.1128/AAC.29.1.99.
29. Manca, C. et al. (1999) 'Mycobacterium tuberculosis catalase and peroxidase activities and resistance to oxidative killing in human monocytes in vitro', Infection and immunity, 67(1), pp. 74–79. Available at: https://doi.org/10.1128/IAI.67.1.74-79.1999.
30. Manni, M. et al. (2021) 'BUSCO Update: Novel and Streamlined Workflows along with Broader and Deeper Phylogenetic Coverage for Scoring of Eukaryotic, Prokaryotic, and Viral Genomes', Molecular Biology and Evolution, 38(10), pp. 4647–4654. Available at: https://doi.org/10.1093/MOLBEV/MSAB199.
31. Mazel, D. (2006) 'Integrons: agents of bacterial evolution', Nature Reviews Microbiology 2006 4:8, 4(8), pp. 608–620. Available at: https://doi.org/10.1038/nrmicro1462.
32. McClure, C.D. and Schiller, N.L. (1996) 'Inhibition of macrophage phagocytosis by Pseudomonas aeruginosa rhamnolipids in vitro and in vivo', Current microbiology, 33(2), pp. 109–117. Available at: https://doi.org/10.1007/S002849900084.
33. Meldrum, A.J. (no date) 'Regulation of Pyoverdine Biosynthesis in Pseudomonas aeruginosa'.
34. Mendes, R.E. et al. (2007) 'Rapid Detection and Identification of Metallo-β-Lactamase-Encoding Genes by Multiplex Real-Time PCR Assay and Melt Curve Analysis', Journal of Clinical Microbiology, 45(2), p. 544. Available at: https://doi.org/10.1128/JCM.01728-06.
35. Mikheenko, A. et al. (2018) 'Versatile genome assembly evaluation with QUAST-LG', Bioinformatics, 34(13), pp. i142–i150. Available at: https://doi.org/10.1093/BIOINFORMATICS/BTY266.
36. Moura, A. et al. (2009) 'INTEGRALL: a database and search engine for integrons, integrases and gene cassettes', Bioinformatics (Oxford, England), 25(8), pp. 1096–1098. Available at: https://doi.org/10.1093/BIOINFORMATICS/BTP105.
37. Nordmann, P., Poirel, L. and Dortet, L. (2012) 'Rapid Detection of Carbapenemase-producing Enterobacteriaceae', Emerging Infectious Diseases, 18(9), p. 1503. Available at: https://doi.org/10.3201/EID1809.120355.
38. Papa-Ezdra, R. et al. (2023) 'Novel Resistance Regions Carrying TnaphA6, blaVIM-2, and blaPER-1, Embedded in an ISPa40-Derived Transposon from Two Multi-Resistant Pseudomonas aeruginosa Clinical Isolates', Antibiotics, 12(2), p. 304. Available at: https://doi.org/10.3390/ANTIBIOTICS12020304/S1.
39. Papagiannitsis, C.C. et al. (2017) 'Molecular Characterization of Carbapenemase-Producing Pseudomonas aeruginosa of Czech Origin and Evidence for Clonal Spread of Extensively Resistant Sequence Type 357 Expressing IMP-7 Metallo-β-Lactamase', Antimicrobial Agents and Chemotherapy, 61(12). Available at: https://doi.org/10.1128/AAC.01811-17.
40. Parks, D.H. et al. (2015) 'CheckM: assessing the quality of microbial genomes recovered from isolates, single cells, and metagenomes', Genome Research, 25(7), pp. 1043–1055. Available at: https://doi.org/10.1101/GR.186072.114.
41. Petrova, A. et al. (2019) 'First detected OXA-50 carbapenem-resistant clinical isolates Pseudomonas aeruginosa from Bulgaria and interplay between the expression of main efflux pumps, OprD and intrinsic AmpC', Journal of medical microbiology, 68(12), pp. 1723–1731. Available at: https://doi.org/10.1099/JMM.0.001106/CITE/REFWORKS.
42. Pilato, V. Di et al. (2019a) 'Identification of a novel plasmid lineage associated with the dissemination of metallo-β-lactamase genes among pseudomonads', Frontiers in Microbiology, 10, p. 464887. Available at: https://doi.org/10.3389/FMICB.2019.01504/BIBTEX.
43. Pilato, V. Di et al. (2019b) 'Identification of a novel plasmid lineage associated with the dissemination of metallo-β-lactamase genes among pseudomonads', Frontiers in Microbiology, 10, p. 1504. Available at: https://doi.org/10.3389/fmicb.2019.01504.
44. Poirel, L., Naas, T. and Nordmann, P. (2006) 'Pyrosequencing as a rapid tool for identification of GES-type extended-spectrum beta-lactamases', Journal of clinical microbiology, 44(8), pp. 3008–3011. Available at: https://doi.org/10.1128/JCM.02576-05.
45. Pottier, M. et al. (2023) 'A 10-year microbiological study of Pseudomonas aeruginosa strains revealed the circulation of populations resistant to both carbapenems and quaternary ammonium compounds', Scientific Reports 2023 13:1, 13(1), pp. 1–16. Available at: https://doi.org/10.1038/s41598-023-29590-0.
46. Quale, J. et al. (2006) 'Interplay of Efflux System, ampC, and oprD Expression in Carbapenem Resistance of Pseudomonas aeruginosa Clinical Isolates', Antimicrobial Agents and Chemotherapy, 50(5), p. 1633. Available at: https://doi.org/10.1128/AAC.50.5.1633-1641.2006.
47. Recio, R. et al. (2020) 'Predictors of Mortality in Bloodstream Infections Caused by Pseudomonas aeruginosa and Impact of Antimicrobial Resistance and Bacterial Virulence', Antimicrobial Agents and Chemotherapy, 64(2). Available at: https://doi.org/10.1128/AAC.01759-19.
48. Roberts, A.P. et al. (2008) 'Revised Nomenclature for Transposable Genetic Elements', Plasmid, 60(3), pp. 167–173. Available at: https://doi.org/10.1016/J.PLASMID.2008.08.001.

49. Robertson, J. and Nash, J.H.E. (2018) 'MOB-suite: software tools for clustering, reconstruction and typing of plasmids from draft assemblies', Microbial Genomics, 4(8). Available at: https://doi.org/10.1099/MGEN.0.000206.
50. Rodríguez-Martínez, J.M., Poirel, L. and Nordmann, P. (2009) 'Molecular Epidemiology and Mechanisms of Carbapenem Resistance in Pseudomonas aeruginosa', Antimicrobial Agents and Chemotherapy, 53(11), p. 4783. Available at: https://doi.org/10.1128/AAC.00574-09.
51. Ross, K. et al. (2021) 'TnCentral: a Prokaryotic Transposable Element Database and Web Portal for Transposon Analysis', mBio, 12(5). Available at: https://doi.org/10.1128/MBIO.02060-21.
52. Russell, A.B. et al. (2013) 'Diverse type VI secretion phospholipases are functionally plastic antibacterial effectors', Nature, 496(7446), p. 508. Available at: https://doi.org/10.1038/NATURE12074.
53. Ryall, B. et al. (2008) 'Pseudomonas aeruginosa, cyanide accumulation and lung function in CF and non-CF bronchiectasis patients', European Respiratory Journal, 32(3), pp. 740–747. Available at: https://doi.org/10.1183/09031936.00159607.
54. Sakuda, A. et al. (2018) 'Divalent cations increase the conjugation efficiency of the incompatibility P-7 group plasmid pCAR1 among different Pseudomonas hosts', Microbiology (Reading, England), 164(1), pp. 20–27. Available at: https://doi.org/10.1099/MIC.0.000583.
55. Schneider, I. et al. (2008) 'VIM-15 and VIM-16, Two New VIM-2-Like Metallo-β-Lactamases in Pseudomonas aeruginosa Isolates from Bulgaria and Germany', Antimicrobial Agents and Chemotherapy, 52(8), p. 2977. Available at: https://doi.org/10.1128/AAC.00175-08.
56. Schwengers, O. et al. (2021) 'Bakta: Rapid and standardized annotation of bacterial genomes via alignment-free sequence identification', Microbial Genomics, 7(11), p. 000685. Available at: https://doi.org/10.1099/MGEN.0.000685/CITE/REFWORKS.
57. Shukla, S.K. and Rao, T.S. (2017) 'An Improved Crystal Violet Assay for Biofilm Quantification in 96-Well Microtitre Plate', bioRxiv, p. 100214. Available at: https://doi.org/10.1101/100214.
58. Siguier, P. et al. (2006) 'ISfinder: the reference centre for bacterial insertion sequences', Nucleic acids research, 34(Database issue). Available at: https://doi.org/10.1093/NAR/GKJ014.
59. Souza, C.O. et al. (2023) 'Genetic and biochemical characterization of BIM-1, a novel acquired subgroup B1 MBL found in a Pseudomonas sp. strain from the Brazilian Amazon region', The Journal of antimicrobial chemotherapy, 78(6), pp. 1359–1366. Available at: https://doi.org/10.1093/JAC/DKAD077.
60. Strateva, T., Setchanova, L. and Peykov, S. (2021) 'Characterization of a Bulgarian VIM-2 metallo-β-lactamase-producing Pseudomonas aeruginosa clinical isolate belonging to the high-risk sequence type 111', https://doi.org/10.1080/23744235.2021.1934531, 53(11), pp. 883–887. Available at: https://doi.org/10.1080/23744235.2021.1934531.
61. Syed, Y.Y. (2021) 'Cefiderocol: A Review in Serious Gram-Negative Bacterial Infections', Drugs, 81(13), p. 1559. Available at: https://doi.org/10.1007/S40265-021-01580-4.
62. Tansirichaiya, S., Rahman, M.A. and Roberts, A.P. (2019) 'The Transposon Registry', Mobile DNA, 10(1), pp. 1–6. Available at: https://doi.org/10.1186/S13100-019-0182-3/FIGURES/3.
63. Thrane, S.W. et al. (2016) 'Application of whole-genome sequencing data for o-specific antigen analysis and in silico serotyping of pseudomonas aeruginosa isolates', Journal of Clinical Microbiology, 54(7), pp. 1782–1788. Available at: https://doi.org/10.1128/JCM.00349-16/SUPPL_FILE/ZJM999095025SO3.XLSX.
64. Toleman, M.A. et al. (2005) 'Italian metallo-beta-lactamases: a national problem? Report from the SENTRY Antimicrobial Surveillance Programme', The Journal of antimicrobial chemotherapy, 55(1), pp. 61–70. Available at: https://doi.org/10.1093/JAC/DKH512.
65. Tu, Q. et al. (2016) 'Room temperature electrocompetent bacterial cells improve DNA transformation and recombineering efficiency', Scientific reports, 6. Available at: https://doi.org/10.1038/SREP24648.
66. Vasil, M.L. et al. (2009) 'A Complex Extracellular Sphingomyelinase of Pseudomonas aeruginosa Inhibits Angiogenesis by Selective Cytotoxicity to Endothelial Cells', PLOS Pathogens, 5(5), p. e1000420. Available at: https://doi.org/10.1371/JOURNAL.PPAT.1000420.
67. Walsh, T.R. et al. (2005) 'Metallo-β-lactamases: The quiet before the storm?', Clinical Microbiology Reviews, 18(2), pp. 306–325. Available at: https://doi.org/10.1128/CMR.18.2.306-325.2005/ASSET/1879A073-59B5-4686-BE7F-2512B2959689/ASSETS/GRAPHIC/ZCM0020521330004.JPEG.
68. Walter, M. V, Porteous, A. and Seidler, R.J. (1987) 'Measuring Genetic', 53(1), pp. 105–109.
69. Wang, M.G. et al. (2021) 'Retrospective Data Insight into the Global Distribution of Carbapenemase-Producing Pseudomonas aeruginosa', Antibiotics, 10(5). Available at: https://doi.org/10.3390/ANTIBIOTICS10050548.
70. Watanabe, M. et al. (1991) 'Transferable imipenem resistance in Pseudomonas aeruginosa', Antimicrobial Agents and Chemotherapy, 35(1), pp. 147–151. Available at: https://doi.org/10.1128/AAC.35.1.147.
71. Wei, Q. et al. (2011) 'Transcription of integron-harboured gene cassette impacts integration efficiency in class 1 integron', Molecular Microbiology, 80(5), pp. 1326–1336. Available at: https://doi.org/10.1111/J.1365-2958.2011.07648.X.

72. Wi, Y.M. et al. (2018) 'Activity of Ceftolozane-Tazobactam against Carbapenem-Resistant, Non-Carbapenemase-Producing Pseudomonas aeruginosa and Associated Resistance Mechanisms', Antimicrobial Agents and Chemotherapy, 62(1). Available at: https://doi.org/10.1128/AAC.01970-17.
73. Wick, R.R. and Holt, K.E. (2022) 'Polypolish: Short-read polishing of long-read bacterial genome assemblies', PLOS Computational Biology, 18(1), p. e1009802. Available at: https://doi.org/10.1371/JOURNAL.PCBI.1009802.
74. Zavascki, A.P. et al. (2006) 'The influence of metallo-β-lactamase production on mortality in nosocomial Pseudomonas aeruginosa infections', Journal of Antimicrobial Chemotherapy, 58(2), pp. 387–392. Available at: https://doi.org/10.1093/JAC/DKL239.
75. Zhao, W.H. and Hu, Z.Q. (2010) 'β-Lactamases identified in clinical isolates of Pseudomonas aeruginosa', http://dx.doi.org/10.3109/1040841X.2010.481763, 36(3), pp. 245–258. Available at: https://doi.org/10.3109/1040841X.2010.481763.
76. Zhao, W.H. and Hu, Z.Q. (2011) 'IMP-type metallo-β-lactamases in Gram-negative bacilli: distribution, phylogeny, and association with integrons', Critical reviews in microbiology, 37(3), pp. 214–226. Available at: https://doi.org/10.3109/1040841X.2011.559944.
77. Zimin, A. V. and Salzberg, S.L. (2020) 'The genome polishing tool POLCA makes fast and accurate corrections in genome assemblies', PLOS Computational Biology, 16(6), p. e1007981. Available at: https://doi.org/10.1371/JOURNAL.PCBI.1007981.
78. Zulianello, L. et al. (2006) 'Rhamnolipids Are Virulence Factors That Promote Early Infiltration of Primary Human Airway Epithelia by Pseudomonas aeruginosa', Infection and Immunity, 74(6), p. 3134. Available at: https://doi.org/10.1128/IAI.01772-05.